Journal of Materials Chemistry A

Accepted Manuscript

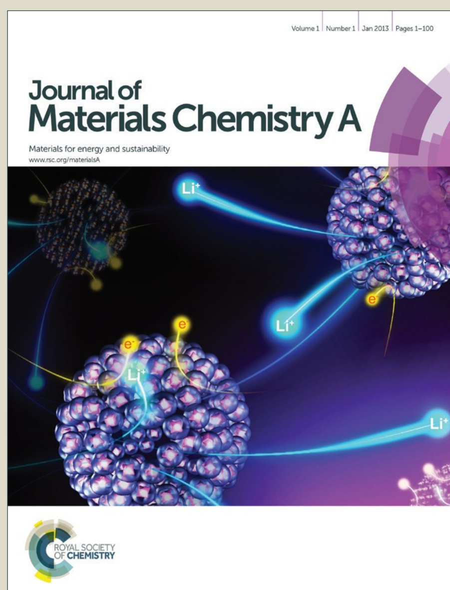

This is an *Accepted Manuscript*, which has been through the Royal Society of Chemistry peer review process and has been accepted for publication.

Accepted Manuscripts are published online shortly after acceptance, before technical editing, formatting and proof reading. Using this free service, authors can make their results available to the community, in citable form, before we publish the edited article. We will replace this *Accepted Manuscript* with the edited and formatted *Advance Article* as soon as it is available.

You can find more information about *Accepted Manuscripts* in the Information for Authors.

Please note that technical editing may introduce minor changes to the text and/or graphics, which may alter content. The journal's standard Terms & Conditions and the Ethical guidelines still apply. In no event shall the Royal Society of Chemistry be held responsible for any errors or omissions in this *Accepted Manuscript* or any consequences arising from the use of any information it contains.

ROYAL SOCIETY OF CHEMISTRY

www.rsc.org/materialsA

Dynamic Article Links ►

Cite this: DOI: 10.1039/c0xx00000x

www.rsc.org/xxxxxx

ARTICLE TYPE

Enhancement of thermoelectric performance of β-Zn_4Sb_3 through resonant distortion of electronic density of states doped with Gd

Baojin Ren,[a] Mian Liu,[a] Xiaoguang Li,[b] Xiaoying Qin,[1a] Di Li,[a] Tianhua Zou,[a] Guolong Sun,[a] Yuanyue Li,[a] Hongxing Xin,[a] and Jian Zhang[a]

5

Journal of Materials Chemistry A Accepted Manuscript

[1]Correspondence author. E-mail: xyqin@issp.ac.cn. Tel: +86 0551 65592750. Fax: +86 0551 65591434.

Cite this: DOI: 10.1039/c0xx00000x

www.rsc.org/xxxxxx

ARTICLE TYPE

The thermoelectric properties of Gd-doped β-Zn_4Sb_3 are investigated. The results indicates that Gd-doping not only causes 41 μVK^{-1} increase in thermopower owing to resonant distortion of DOS but also results in ~14% reduction in thermal conductivity at doping content of 0.2%. Consequently, a largest ZT=1.2 is achieved at 655 K.

Introduction

Recently, thermoelectric materials have attracted a great deal of attention for their possible applications in energy conversion and power generation.[1-5] However, their applications are limited by the relatively low conversion efficiency, which is quantified by thermoelectric figure of merit, $ZT=(S^2/\rho\kappa)T$, where ρ, S and κ is the electrical resistivity, the thermopower, and the total thermal conductivity. β-Zn_4Sb_3 is a very potential thermoelectric material in the moderate temperature range because it possesses high thermoelectric performance[6] and is made of relatively cheap and nontoxic elements. In order to improve its thermoelectric properties, doping approach was used to optimize its carrier concentration and reduce its thermal conductivity. For instance, doping of Pb, Bi, Nb, Cu, Cd, Co, Sn, In, Al, Ga, Mg, Ge and Hg[7-19] have been investigated so far. The results showed that, however, only a small amount doping of one of these elements could lead to limited improvement of its thermoelectric performance. The main reasons would lie in the factors: (i) thermal conductivity of β-Zn_4Sb_3 is very low (< 1 W $m^{-1}K^{-1}$)[6, 20] which is close to the lower limit for the thermal conductivity in solids; (ii) the hole concentration of pristine β-Zn_4Sb_3 is already close to the optimum (in the order of 10^{18}-10^{19} cm^{-3}).[6, 16] These characters of β-Zn_4Sb_3 suggest that it is difficult to enhance its thermoelectric performance through conventional doping, unless themopower S can be extra elevated upon doping.

Recently, Heremans *et al.*[21] found that doping can give rise to resonant distortion of electronic density of state through the use of the thallium impurity levels in PbTe, resulting in enhancement of its ZT. According to Mahan Sofo theory,[22] the local increase in the density of state g(E) (DOS) can strengthen thermopower (S). The effect of this local increase in DOS on S is given by the Mott expression (Eq.1).

$$S=\frac{\pi^2}{3}\frac{k_B}{q}k_BT\left\{\frac{d[\ln(\sigma(E))]}{dE}\right\}_{E=E_f}$$
$$=\frac{\pi^2}{3}\frac{k_B}{T}k_BT\left\{\frac{1}{p}\frac{dp(E)}{dE}+\frac{1}{\mu}\frac{d\mu(E)}{dE}\right\}_{E=E_f} \quad . \quad (1)$$

Here, S depends on the energy-dependent electrical conductivity $\sigma(E)=p(E)q\mu(E)$ taken at the Fermi energy E_f,[23] with $p(E)=g(E)f(E)$, where p(E) is the carrier concentration, f(E) is the Fermi function, q the carrier charge, and μ(E)the mobility. Eq. 1 shows that an increased energy dependence of p(E), for instance by a local increase in DOS g(E), can enhance thermopower. Very recently, our group[24-26] found that rare earth element doping can significantly improve thermopower of β-Zn_4Sb_3, which could be ascribed to the occurrence of the resonant distortion of DOS.

In the present work, rare earth Gd was chosen as a dopant to explore possible resonant distortion of DOS in β-Zn_4Sb_3. Our results show that besides large reduction of thermal conductivity κ, thermopower S of Gd doped compound β-$(Zn_{1-x}Gd_x)_4Sb_3$ increases by ~40 μVK^{-1} as x=0.002 and 0.003; meanwhile, density-of-states effective mass of β-Zn_4Sb_3 is estimated to be around 1.3-1.7 times larger than that of the un-doped one, signifying the occurrence of resonant distortion of DOS, which is verified low-temperature (<4 K) specific heat. Our first-principles calculations further reveals that the resonant distortion near edge of the valence band originates mainly from contribution of d-electrons of Gd. Due to both enhanced S and reduced κ, a largest ZT of 1.2 (at 655 K) is achieved for β-$(Zn_{1-x}Gd_x)_4Sb_3$ (x=0.002) at 655 K, which is around 1.6 times larger than that of the un-doped sample.

Experimental Procedures

β-$(Zn_{1-x}Gd_x)_4Sb_3$ (x=0, 0.001, 0.002 and 0.003) compounds were synthesized by the melting and hot-pressing method (~95% theoretical density). The phase structures of the obtained samples were determined by using X-ray diffraction (XRD) with Cu Kα radiation (λ=1.540598Å). Accuracy lattice parameters were measured with XRD by using a Si standard for calibration. The thermal conductivity κ was calculated using the relationship $\kappa=\alpha C_p\rho$, in which thermal diffusivity α measured by laser flash

Journal of Materials Chemistry A Accepted Manuscript

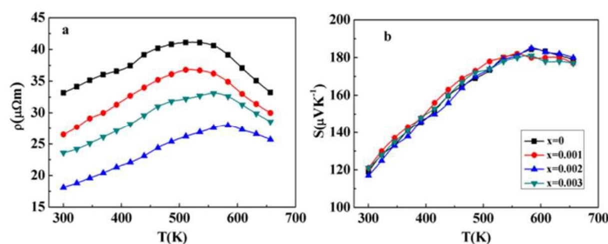

Fig. 1 Temperature dependence of (a) electrical resistivity and (b) thermopower for β-$(Zn_{1-x}Gd_x)_4Sb_3$ (x=0, 0.001,0. 002 and 0.003) compounds.

method (LFA 457) in Ar atmosphere from 300 K to 655 K, the heat capacity C_p was measured with a Perkin Elmer Diamond DSC, and density ρ was measured in ethanol by using Archimedes' method. The electrical resistivity and thermopower were measured simultaneously using the standard four-probe method (ZEM-3) in He atmosphere from 300K to 655K. The Hall coefficients and low-temperature heat capacity were measured by using a physical property measurement system (PPMS, Quantum Design) at 300K and 2-4 K, respectively.

Computational methods

Although β-Zn_4Sb_3 was already discovered and studied for decades, a complete view on its true crystal structure was presented only recently.[27-29] Cargnoni *et al*[30]. had proposed a recognized model consists of three types of structures to simplify the practical structure, it was noted that the three types of structures have very similar DOS regardless of the zinc content and structure.[31] Hence, for simplicity, we utilized the crystal structure of a hypothetical disorder-free β-Zn_4Sb_3 with a framework of $Zn_{36}Sb_{30}$, one of basic structures in Cargnoni's model. Then ab initio electrical structure calculations were carried out for the Zn-substituted compounds $GdZn_{35}Sb_{30}$.

Our calculations are performed within the framework of the density-functional theory, with the PBE generalized gradient approximation to the exchange correlation energy, and the valence electron interaction was modeled by the projector augmented wave potential, as implemented in the Vienna ab initio simulation package (VASP).[32-34] The plane wave cut off and k-point density, obtained using the Monkhorst–Pack method. Structural relaxations have been performed by using the conjugate gradient algorithm. The ionic coordinates and the unit cell's size and shape were optimized simultaneously to eliminate structures with internal stress.

Results and Discussion

The phase of β-$(Zn_{1-x}Gd_x)_4Sb_3$ (x=0, 0.001, 0.002 and 0.003) are analyzed with XRD at room temperature. All diffraction peaks perfectly correspond to β-Zn_4Sb_3 (JCPD No. 89–1969) phase, no obvious impurity phase being detected. With increasing Gd content x from 0 to 0.003, the lattice constant a and c increases monotonically as shown in Table I, evidencing that Gd has substituted for Zn to form substitutional compounds, for ionic radius of Gd^{3+} is 1.05 Å, which is larger than that (0.74 Å) of Zn^{2+}, leading to expansion of the host lattice.

The electrical resistivity and thermopower versus temperature for β-$(Zn_{1-x}Gd_x)_4Sb_3$ (x=0, 0.001, 0.002 and 0.003) samples in the temperature range of 300 -655 K are depicted in Fig.1. One can see from Fig. 1(a) that the temperature dependence of ρ for all samples is similar: it initially increases with increasing temperature and then decreases with further increase in temperature. This reduction of ρ at high temperatures can be ascribed to thermal excitation of minority carriers. Moreover, ρ decreases with increasing Gd content (except for the sample with x=0.003). Especially, the resistivity of $(Zn_{0.998}Gd_{0.002})_4Sb_3$ decreases to 18.8 μΩm at 300K, which is 45% lower than that (34.2 μΩm) of the un-doped sample. The highest ρ value for un-doped sample appears at T_p~525 K, while this peak temperature T_p shifts to higher temperature for the doped samples, particularly, T_p appears at 575 K for x=0.002, suggesting that Gd doping can inhibits the thermal excitation of minority carriers to some degree.

In contrast, thermopower S for compounds does not change obviously with Gd content in the whole temperature range investigated (Fig. 1(b)). The positive values of S indicate that the major charge carriers are holes in all samples. The un-doped and doped samples have $S \approx 120$ μVK^{-1} at RT and almost increase linearly to 180 μVK^{-1} with increasing temperature below ~ 575 K, and then show weak temperature dependence with small reduction with further increasing temperature.

The positive Hall coefficient R_H is for β-$(Zn_{1-x}Gd_x)_4Sb_3$ (x=0, 0.001, 0.002 and 0.003) indicates hole conduction in this system, being consistent with the results of S data. Assuming parabolic bands and a single band conduction process at 300 K, the obtained hole concentration p is 8.0×10^{19}, 11.4×10^{19}, 17.6×10^{19}, and 14.0×10^{19} cm^{-3} as x increases from 0 to 0.001, 0.002, and

Journal of Materials Chemistry A Accepted Manuscript

then 0.003, respectively, as shown in Table I. As we know, β-Zn_4Sb_3 is a p-type semiconductor and has two kinds of Zn sites in

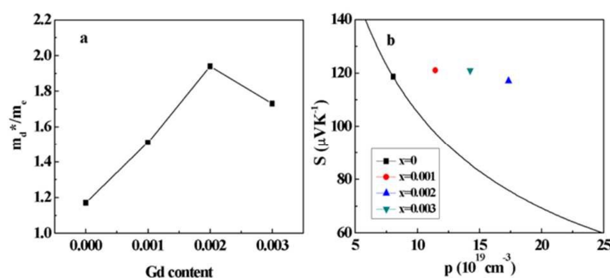

Fig. 2 (a) the ratio of density of states effective mass m_d* to that of the free electron at 300K, (b) variation of thermopower with carrier concentration for β-$(Zn_{1-x}Gd_x)_4Sb_3$ (x=0, 0.001,0. 002 and 0.003) compounds. The solid line is carrier concentration dependence of thermopower for the un-doped β-Zn_4Sb_3, which is calculated by using formulae (2) and (3) for m_d* =1.17m_e.

its framework: lattice Zn sites (among which Zn occupancy is ~90%) and interstitial Zn sites.[30] In other words, its carriers (holes) come from vacancies in Zn lattice sites. Gd-doping will affect vacancy content, which eventually leads to the changes of the carrier concentration: the more of the vacancies, the more of the holes. Hence, as Gd content x=0.001 and 0.002, the carrier concentration increase, indicating that the number of Zn vacancies increases, and this increased vacancies can scattering phonons, leading to decrease of the lattice thermal conductivity (see Fig. S2). However, for the sample with x=0.003, hole concentration decreases, which indicate that the number of Zn vacancies decreases.

The measurements of carrier concentration indicate that the decrease in resistivity ρ for the doped samples originates from the increase in carrier concentration. An interesting phenomenon one notices here is that there is no reduction in S (seen in Fig. 1(b)) for dope samples though p increases, which seems to be in conflict with Mott equation (Eq. 1), which implies other physics mechanism works. By using a single parabolic band model, the density state effective mass m_d* and S can be expressed as:[6]

$$m_d* = \frac{h^2}{2k_B T}\left(\frac{p}{4\pi F_{1/2}(\xi_F)}\right)^{2/3}, \qquad (2)$$

$$S = \frac{k_B}{e}\left[\frac{[(r+\frac{5}{2})F_{r+\frac{3}{2}}(\xi_F)]}{[(r+\frac{3}{2})F_{r+\frac{1}{2}}(\xi_F)]} - \xi_F\right] = \frac{k_B}{e}\left[\frac{2F_1(\xi_F)}{F_0(\xi_F)} - \xi_F\right], \qquad (3)$$

with Fermi integral of order i,

$$F_i(\xi_F) = \int_0^\infty \frac{x^i}{1+e^{(x-\xi_F)}}dx. \qquad (4)$$

Here k_B is the Boltzmann constant, h is Plank constant, and ζ_F is the reduced Fermi level (E_f/k_BT). In our calculations, we assume acoustic phonon scattering dominates (i.e., r=-1/2) in the compounds and use the experimental data of the p and S. The density of state effective mass m_d* for all the samples can be calculated and the obtained effective mass m_d*/m_e (where m_e is the free electron mass) at 300 K is shown in Fig. 2(a). m_d* of β-$(Zn_{1-x}Gd_x)_4Sb_3$ reaches 1.51m_e, 1.94m_e, and 1.73m for x=0.001, 0.002 and 0.003, which is 1.3, 1.7 and 1.5 times larger than that of the un-doped sample, respectively (It should be pointed out that the calculated effective mass m_d* (at 300 K) for un-doped β-Zn_4Sb_3 is 1.17 m_e that agree well with the result (1.18m_e) reported by Caillat *et al.*[6]). This increase in m_d* actually signify the increase in DOS. That is, the increase in m_d* implies a non-parabolic perturbation in the electron dispersion relations, i.e. resonant distortion of DOS of β-Zn_4Sb_3 near Fermi level. In fact, Gd doping result in 41 μV/K and 36 μV/K increase in thermopower at 300K for the doped compounds with x=0.002 and 0.003, respectively, as shown in Fig. 2(b), where the solid line shows the dependence of S on carrier concentration calculated using formulae (2) and (3) and m_d*=1.17m_e for β-Zn_4Sb_3, indicating that all the data of S with different Gd content would fall on this line if there were no other mechanism (i.e. local resonant distortion of DOS) functions upon Gd doping.

To verify resonance distortion of DOS occurring in the doped compounds β-$(Zn_{1-x}Gd_x)_4Sb_3$ (x≠0), low temperature (< 4 K) heat capacity C_p were measured for both un-doped β-Zn_4Sb_3 and the doped compounds. As is well known, low temperature (< 4 K) heat capacity C_p for a solid has a temperature dependence: $C_p=\gamma T+bT^3$, in which the term bT^3 stands for the lattice contribution and γT is the contribution from charge carriers with γ

Journal of Materials Chemistry A Accepted Manuscript

 This journal is © The Royal Society of Chemistry [year]

being related to $N(E_f)$ (here $N(E_f)$ is electronic DOS at the Fermi level):

$$\gamma = \frac{\pi^2}{3} k_B^2 N(E_f)\,. \qquad (5)$$

However, in the Gd-doped samples magnetic heat capacity C_m from 4f electrons of Gd cannot be ignored. Then, the total heat capacity can be written as: $C_p = \gamma T + bT^3 + C_m$. According to the work of M.J. Parsons *et al.*,[35, 36] magnetic heat capacity C_m for

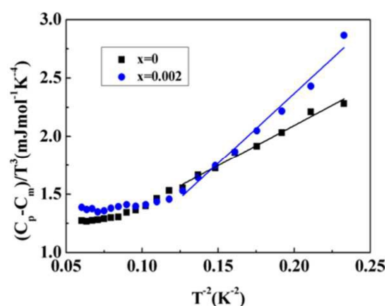

Fig. 3 The plots of $(C_p\text{-}C_m)/T^3$ vs. T^{-2} for β-$(Zn_{1-x}Gd_x)_4Sb_3$ (x=0 and 0.002) compounds.

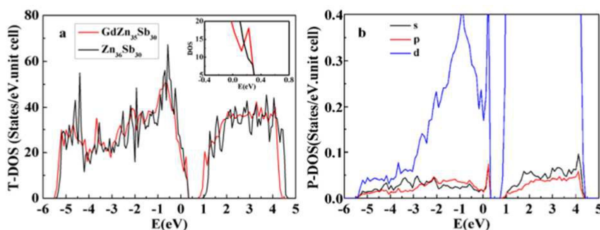

Fig. 4 (a) The total DOS (T-DOS) of $Zn_{36}Sb_{30}$ and $GdZn_{35}Sb_{30}$, and (b) Gd partial DOS (P-DOS). The energy is in respect to the host valence band maximum.

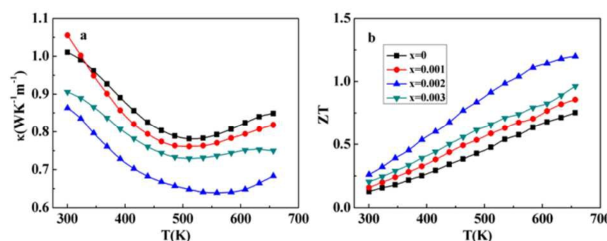

Fig. 5 Temperature dependence of (a) total thermal conductivity κ and (b) ZT for β-$(Zn_{1-x}Gd_x)_4Sb_3$ (x=0, 0.001,0. 002 and 0.003) compounds.

Gd-doped sample with x=0.002, at T<9 K, can derived as C_m=3.6T(mJ/mol K) (see Supplemental material). By subtracting C_m from Cp one has $C_p\text{-}C_m = \gamma T + bT^3$ for th eGd-doped samples. Hence, the slope of a plot C_p/T^3 (or $(C_p\text{-}C_m)/T^3$) vs. $1/T^2$ gives γ that reflect directly values of DOS at the Fermi level. Fig. 3 shows the plots of C_p/T^3 vs. $1/T^2$ for an un-doped β-Zn_4Sb_3 and a typical doped compound β-$(Zn_{1-x}Gd_x)_4Sb_3$ (x=0.002) (where $(C_p\text{-}C_m)/T^3$ vs. $1/T^2$ is plotted). One can see that the slope (γ) of the plot $(C_p\text{-}C_m)/T^3$ vs. $1/T^2$ for the doped compound β-$(Zn_{0.998}Gd_{0.002})_4Sb_3$ is substantially larger than that for the un-doped one. By linear fitting of the curves in the low temperature regime, one obtains the ratio $\gamma_{dop}/\gamma_{un\text{-}dop}=N(E_f)_{dop}/N(E_f)_{0un\text{-}dop}=$ ~1.91, which is in good agreement with the ratio of density of states effective mass (see Fig.2a), revealing that Gd doping indeed causes great increase in DOS near Fermi level of the compound.

Our experimental observations are further confirmed by our theoretical calculations (Fig. 4). One can see from Fig. 4(a) that as compared with DOS of the pristine β-Zn_4Sb_3, there is a sharp peak appearing in the DOS and near the edge of valence-band for the Gd doping β-Zn_4Sb_3 (see inset in Fig. 4(a)). Partial DOS analysis indicates that the resonant distortion of DOS of the Gd doped β-Zn_4Sb_3 comes mainly from contribution of d-sate of Gd (Fig. 4(b)), other than small contribution from p- and s-states. Present result indicate clearly that Gd doping causes resonant distortion of DOS of β-Zn_4Sb_3, which will result in enhancement of m* and thermopower, which is in good agreement with our experimental result.

The temperature behavior of total thermal conductivity for $(Zn_{1-x}Gd_x)_4Sb_3$ (x=0, 0.001, 0.002 and 0.003) are plotted in Fig. 5(a). In addition to the enhancement of thermopower through resonant distortion of DOS, Gd doping also causes substantial decrease in κ in the measured temperature range. Thermal conductivity for all the samples initially decreases with increasing temperature and then increases with further increasing temperature. At 300 K, the sample with x=0.002 and 0.003 reduces to 0.86 $Wm^{-1}K^{-1}$ and 0.91 $Wm^{-1}K^{-1}$, respectively, which is ~15% and ~10% smaller than that (1.01 $Wm^{-1}K^{-1}$) of the un-doped one. To determine the electronic component of the thermal conductivity, the Lorenz number L was estimated using formulae (6) with the assumption of transport dominated by acoustic scattering and a single parabolic band.[37]

$$L = \left(\frac{k_B}{e}\right)^2 \frac{3F_0(\xi_F)F_2(\xi_F) - 4F_1(\xi_F)^2}{F_0(\xi_F)^2}\,. \qquad (6)$$

Journal of Materials Chemistry A Accepted Manuscript

The obtained values of L is 1.48-1.49 × 10^{-8} V^2K^{-2}, as list in Table I. Therefore, κ_L can be obtained by subtracting κ_c (κ=κ_L+κ_c). As shown in Fig. S2, κ_L decreases with increasing doping content of Gd (except x=0.003) due to phonon scattering of impurity (Gd) and increased Zn vacancies. As mentioned above, the hole concentration deceases for sample with x=0.003, which suggests that the number of Zn vacancies decreases. Hence, the abnormal increase of κ for the sample with x=0.003 as compared to that for x=0.002 could be caused by the reduced Zn vacancies in lattice sites, which should cause increase of the lattice conductivity due to weakened phonon scattering.

Fig. 5(b) gives the dimensionless figure of merit, ZT, for all samples as functions of temperature. The behavior of ZT for the four samples is similar: it increases with increasing temperature, and reaches the maximum value at 655 K. As a result of enhancement of thermopower and reduction in thermal conductivity, the largest ZT of 1.2 sample is achieved for β-$(Zn_{0.998}Gd_{0.002})_4Sb_3$, which is ~60% larger than the un-doped sample (ZT=0.75).

Conclusions

In summary, our experimental studies indicate that Gd-doping causes resonant distortion of DOS near Fermi level of β-$(Zn_{1-x}Gd_x)_4Sb_3$, which is manifested by large increase in DOS effective mass and verified by low-temperature heat capacity. First-principles calculations further reveal that a high sharp resonant peak in the DOS locating near the valence band maximum of β-Zn_4Sb_3 originates largely from contribution of d-orbit of Gd. This resonant distortion of DOS results in an increase of thermopower by ~40 μVK^{-1} for β-$(Zn_{1-x}Gd_x)_4Sb_3$ (x=0.002 and 0.003); additionally, this Gd-doping gives rise to ~15% reduction of thermal conductivity κ at x=0.002 content. As a result, a largest value of ZT=1.2 is achieved at 655 K for β-$(Zn_{1-x}Gd_x)_4Sb_3$ (x=0.002), which is ~60% larger than that (ZT=0.75) of the un-doped one. Present result demonstrates that Gd doping is a promising way to elevating thermoelectric performance of β-Zn_4Sb_3 via bringing about resonant distortion of DOS.

Acknowledgments

Financial support from National Natural Science Foundation of China (Nos. 11374306, 11174292, 51101150, 50972146, and 10904144) was gratefully acknowledged.

Notes and references

[a] *Key Laboratory of Materials Physics, Institute of Solid State Physics, Chinese Academy of Science,230031 Hefei, P. R. China.*

[b] *Hefei National Laboratory for Physical Sciences at Microscale, Department of Physics, University of Science and Technology of China, 230026 Hefei, P. R. China.*

1. B. C. Sales, D. Mandrus and R. K. Williams, *Science*, 1996, **272**, 1325-1328.
2. G. Mahan, B. Sales and J. Sharp, *Phys Today*, 1997, **50**, 42-47.
3. T. C. Harman, P. J. Taylor, M. P. Walsh and B. E. LaForge, *Science*, 2002, **297**, 2229-2232.
4. G. Chen, M. S. Dresselhaus, G. Dresselhaus, J. P. Fleurial and T. Caillat, *International Materials Reviews*, 2003, **48**, 45-66.
5. G. J. Snyder and E. S. Toberer, *Nat Mater*, 2008, **7**, 105-114.
6. T. Caillat, J. P. Fleurial and A. Borshchevsky, *J Phys Chem Solids*, 1997, **58**, 1119-1125.
7. T. Caillat and J. P. Fleurial, *Proc Iecec*, 1996, 905-909.
8. J. L. Cui, H. Fu, D. Y. Chen, L. D. Mao, X. L. Liu and W. Yang, *Mater Charact*, 2009, **60**, 824-828.
9. J. L. Cui, L. D. Mao, D. Y. Chen, X. Qian, X. L. Liu and W. Yang, *Current Applied Physics*, 2009, **9**, 713-716.
10. T. Koyanagi, K. Hino, Y. Nagamoto, H. Yoshitake and K. Kishimoto, *Proceedings Ict'97 - Xvi International Conference on Thermoelectrics*, 1997, 463-466.
11. D. Li, H. H. Hng, J. Ma and X. Y. Qin, *J Mater Res*, 2009, **24**, 430-435.
12. A. P. Litvinchuk, J. Nylén, B. Lorenz, A. M. Guloy and U. Häussermann, *Journal of Applied Physics*, 2008, **103**, 123524.
13. F. Liu, X. Y. Qin and H. X. Xin, *Journal of Physics D: Applied Physics*, 2007, **40**, 7811-7816.
14. G. Nakamoto, T. Souma, M. Yamaba and M. Kurisu, *Journal of Alloys and Compounds*, 2004, **377**, 59-65.
15. B. L. Pedersen, H. Birkedal, E. Nishibori, A. Bentien, M. Sakata, M. Nygren, P. T. Frederiksen and B. B. Iversen, *Chem Mater*, 2007, **19**, 6304-6311.
16. S.-C. Ur, I.-H. Kim and P. Nash, *Materials Letters*, 2004, **58**, 2132-2136.
17. B. L. Pedersen, H. Birkedal, M. Nygren, P. T. Frederiksen and B. B. Iversen, *Journal of Applied Physics*, 2009, **105**.
18. B. L. Pedersen, H. Yin, H. Birkedal, M. Nygren and B. B. Iversen, *Chem Mater*, 2010, **22**, 2375-2383.
19. S. Y. Wang, X. J. Tan, G. J. Tan, X. Y. She, W. Liu, H. Li, H. J. Liu and X. F. Tang, *J Mater Chem*, 2012, **22**, 13977-13985.
20. J. Nylen, S. Lidin, M. Andersson, B. B. Iversen, H. X. Liu, N. Newman and U. Haussermann, *Chem Mater*, 2007, **19**, 834-838.
21. J. P. Heremans, V. Jovovic, E. S. Toberer, A. Saramat, K. Kurosaki, A. Charoenphakdee, S. Yamanaka and G. J. Snyder, *Science*, 2008, **321**, 554-557.
22. G. D. Mahan and J. O. Sofo, *Proceedings of the National Academy of Sciences of the United States of America*, 1996, **93**, 7436-7439.
23. M. Cutler and N. F. Mott, *Phys Rev*, 1969, **181**, 1336-&.
24. Q. Q. Wang, X. Y. Qin, D. Li, R. R. Sun, T. H. Zou and N. N. Wang, *Journal of Applied Physics*, 2013, **113**,

Journal of Materials Chemistry A Accepted Manuscript

 This journal is © The Royal Society of Chemistry [year]

124901.
25. Q. Q. Wang, X. Y. Qin, D. Li and T. H. Zou, *Applied Physics Letters*, 2013, **102**, 154101.
26. M. Liu, X. Qin, C. Liu, X. Li and X. Yang, *Journal of Alloys and Compounds*, 2014, **584**, 244-248.
27. A. S. Mikhaylushkin, J. Nylen and U. Haussermann, *Chemistry*, 2005, **11**, 4912-4920.
28. J. Nylen, M. Andersson, S. Lidin and U. Haussermann, *J Am Chem Soc*, 2004, **126**, 16306-16307.
29. Y. A. Ugai, E. M. Averbakh and V. V. Lavrov, *Sov Phys-Sol State*, 1963, **4**, 2393-2395.
30. F. Cargnoni, E. Nishibori, P. Rabiller, L. Bertini, G. J. Snyder, M. Christensen, C. Gatti and B. B. Iversen, *Chemistry*, 2004, **10**, 3861-3870.
31. G. J. Snyder, M. Christensen, E. Nishibori, T. Caillat and B. B. Iversen, *Nat Mater*, 2004, **3**, 458-463.
32. P. E. Blochl, *Phys Rev B*, 1994, **50**, 17953-17979.
33. G. Kresse and D. Joubert, *Phys Rev B*, 1999, **59**, 1758-1775.
34. J. P. Perdew, K. Burke and M. Ernzerhof, *Phys Rev Lett*, 1996, **77**, 3865-3868.
35. M. J. Parsons, J. Crangle, B. Dennis, K. U. Neumann and K. R. A. Ziebeck, *Czech J Phys*, 1996, **46**, 2057-2058.
36. M. J. Parsons, J. Crangle, K. U. Neumann and K. R. A. Ziebeck, *J Magn Magn Mater*, 1998, **184**, 184-192.
37. E. S. Toberer, P. Rauwel, S. Gariel, J. Tafto and G. J. Snyder, *J Mater Chem*, 2010, **20**, 9877-9885.

Author contribution

Baojin Ren synthesized the samples, measured the property and analysed data. Mian Liu contributed to the First-Principles calculations. Xiaoguang Li was responsible for the low-temperature heat capacity. Xiaoying Qin designed the experiments and analysed data. Di Li and Tianhua Zou helped the measurements of thermoelectric properties. Guolong Sun and Jian Zhang contributed to microstructural characterization. Yuanyue Li and Hongxing Xin contributed to the synthesis of compounds.

Table Caption

TABLE I List of room temperature lattice constant (*a* and *c*), carrier concentration (*p*), carrier mobility (μ), and Lorenz number *L* of the bulk samples for β-$(Zn_{1-x}Gd_x)_4Sb_3$ (x=0, 0.001, 0.002, and 0.003) compounds.

x	a (Å)[a]	c (Å)[a]	p(10^{19} cm^{-3})[b]	μ(cm^{-2}/Vs)[c]	L(×10^{-8} V^2K^{-2})[d]
x=0	12.218	12.411	8.0	22.9	1.48
x=0.001	12.217	12.420	11.4	19.8	1.48
x=0.002	12.223	12.421	17.6	18.9	1.49
x=0.003	12.226	12.426	14.0	18.5	1.48

[a] *a* and *c* is the lattice parameters.
[b] *p* is the carrier concentration.
[c] μ is the Hall mobility.
[d] *L* is the Lorenz number.

Journal of Materials Chemistry A Accepted Manuscript